Two-dimensional ordering of chlorine on Ag(100)

David E. Taylor,* Ellen D. Williams,† Robert L. Park, N. C. Bartelt, and T. L. Einstein
Department of Physics and Astronomy, University of Maryland, College Park, Maryland 20742
(Received 2 May 1985)

Chlorine adsorption on Ag(100) saturates at $\frac{1}{2}$ monolayer (ML) in a $c(2\times2)$ structure. Desorption occurs above 650 K without disordering. The sticking coefficient remains constant to within 0.05 ML of saturation, consistent with the existence of a highly mobile precursor to adsorption. The $c(2\times2)$ structure forms at a critical coverage of 0.394 ± 0.007 ML at room temperature. This is slightly higher than the critical coverage of the hard-square model (0.368 ML), suggesting the influence of further-neighbor interactions. The transition to an ordered structure as a function of coverage is second order and the measured critical exponent $\beta/(1-\alpha)$ is 0.12 ± 0.04, consistent with the Ising value of $\frac{1}{8}$.

I. INTRODUCTION

The experimental study of two-dimensional critical phenomena in chemisorbed systems is a relatively new topic, and one of increasing interest. It has been known for some time that mobile, chemisorbed species on clean, single-crystal metal surfaces can form ordered overlayers under certain conditions,[1] and over the years the existence of such ordered overlayers has been reported for an enormous number of systems, one recent reference listing 444.[2] The lattice-gas model can be used to predict the phase diagrams for such systems of atoms adsorbed on surfaces. Comparisons between these model phase diagrams and experimental phase diagrams can be used to draw conclusions about adatom-adatom interactions. In this paper we apply a much studied lattice-gas model—the hard-square model—to chlorine adsorbed on the (100) face of a silver single crystal. Using low-energy electron diffraction (LEED), Auger-electron spectroscopy (AES), and work-function-change measurements, we have studied the temperature-coverage phase diagram for Cl/Ag(100). By comparing this phase diagram with hard-square diagrams we have been able to make inferences about the Cl-Cl interactions.

Previous work has established that Cl dissociates and forms a $c(2\times2)$ structure on Ag(100) for sufficiently high Cl exposures.[3–5] In this structure the Cl is believed to be bonded at the fourfold hollow site of the first layer of Ag atoms[6,7] (Fig. 1). If we assume that this binding site is the only one, we might be able to specify the energy U of a Cl overlayer by specifying the configuration of Cl atoms on the square lattice. Explicitly,

$$U(\{n_i\})=-\mu\sum_i n_i+\sum_{i,j}E_{ij}^{(2)}n_in_j+\sum_{i,j,k}E_{ijk}^{(3)}n_in_jn_k+\cdots, \tag{1}$$

where n_i is the occupancy (0 or 1) of the ith binding site, μ is the chemical potential of the Cl overlayer, $E_{ij}^{(2)}$ are pairwise adatom-adatom interaction energies, $E_{ijk}^{(3)}$ are trio energies, and so on. This is the square lattice-gas model. It implicitly assumes that thermal vibrations and all other degrees of freedom of the substrate-adsorbate system do not interact with the site occupancy degrees of freedom. A simple form of this model, which appears to describe our experimental system quite well, occurs when the nearest-neighbor pairwise interaction energy (E_1 in Fig. 1) is effectively an exclusion for accessible temperatures and pressures. The Cl atoms can then be thought of as hard squares, blocking neighboring sites from occupation. If there were no further-neighbor interactions (an assumption that would be valid at temperatures much greater than all interaction energies except for the nearest-neighbor exclusion), the Cl atoms could be described by the pure hard-square model considered by many authors.[8–13] This athermal model has a continuous order-disorder transition at a coverage (Θ), which is controlled by μ, of approximately 0.368 (Refs. 10 and 13). ($\Theta=0.5$ is the saturation coverage.) At densities less than this Θ_c the system is disordered; at densities greater than Θ_c there is long-range $c(2\times2)$ order. There is strong evidence that this transition is in the Ising universality class, as expected.

At room temperature we observe that Cl/Ag(100) un-

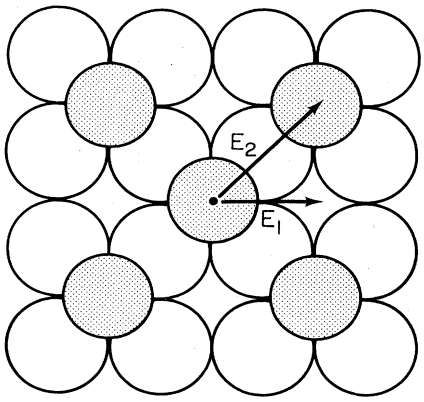

FIG. 1. A schematic picture of the $c(2\times2)$ overlayer formed by Cl on Ag(100). E_1 and E_2 represent the nearest- and next-nearest-neighbor interaction energies.

dergoes a continuous order-disorder transition at a coverage of 0.394 ± 0.007. We find that we can account for the difference between the critical coverage for Cl/Ag(100) and the pure hard-square model by assuming reasonable further-neighbor interactions. For example, the calculations of Kinzel and Schick[13] show that a repulsive second-neighbor interaction energy (E_2 in Fig. 1) would account for the difference.

The remainder of the paper is divided into four sections. In Sec. II details of sample preparation and instrumentation are described. In Sec. III experimental data on the Cl adsorption kinetics, the temperature dependence of the $c(2\times2)$ overlayer, and the changes in the LEED beam profiles through the ordering transition are presented. Analysis and discussion of the experimental results are presented in Sec. IV. In Sec. V the major results and conclusions are summarized.

II. EXPERIMENTAL

Experiments were performed in ultrahigh vacuum (UHV) in a stainless-steel bell jar equipped with a quadrupole mass spectrometer and LEED-AES electron optics. The system also contained provisions for cleaning the sample by Ar^+ ion bombardment. Chlorine, nominally 99.995% pure, was admitted through a conventional variable leak valve. Chlorine exposures are reported in Langmiurs ($1\ \mathrm{L} \equiv 10^{-6}$ torr s) using the uncorrected pressure measured with an ion gauge mounted near the leak valve. The actual exposure at the sample is lower by an unknown amount due to a large sticking coefficient for Cl_2 on the walls of the chamber. The sample temperature was monitored by a Chromel-Alumel thermocouple and could be controlled from 90 to 1000 K.

A spot photometer consisting of a 35-mm camera lens and a photomultiplier tube with a pinhole aperture was used for measuring the LEED beam intensity profiles. A flat mirror was used to position the desired diffraction spot onto the center of the camera lens, which focused an image of the spot onto the pinhole aperture. Beam profiles were measured by sweeping the beam across the aperture by changing the primary energy of the electron gun. The surface parallel component of the wave vector, $k_{||}$, was obtained from

$$k_{||} = \left[\frac{2mE}{\hbar^2}\right]^{1/2} \sin\theta \ , \qquad (2)$$

where E is the electron energy and θ is the angle between the normally incident beam and the diffracted beam.

The silver sample was oriented to within $\frac{1}{3}^\circ$ of the (100) plane. The surface was prepared by a combination of simultaneous mechanical and chemical polishing. A chemical polish of 88% H_2O, 11% CrO_3, and 1% HCl was mixed with 0.05-μm alumina grit, and the silver was mechanically polished with this mixture. The surface was then carefully rubbed with a cotton swab soaked in the chemical polish until the "tears" resulting from mechanical polish just disappeared. The sample was rinsed in boiling, distilled water, followed by a second rinse in acetone and methanol. After this procedure, large areas of the surface appeared perfectly smooth under a 200× microscope. After an initial cycle of sputtering and annealing in UHV, sulfur was the principal contaminant. The sulfur was eliminated by slowly sputtering the hot sample ($T=630\,^\circ$C, $V=250$ V, $I=12\ \mu$A) for 24 h, then annealing in UHV for $\frac{1}{2}$ h at 500 °C. The silver surface, once cleaned, exhibited sharp LEED spots, and proved to be remarkably inert with respect to background gases. AES spectra from a freshly prepared surface could be taken days apart without any noticeable change. This convenient property allowed data collection over runs as long as 8 h without significant surface contamination.

III. RESULTS

A. Adsorption

The Cl/Ag(100) system was examined using LEED, Auger-electron spectroscopy, and work-function measurements. As shown in Fig. 2, the Cl Auger signal increased almost linearly with exposure to Cl_2 at 2×10^{-9} torr until it abruptly saturated at an exposure of about 5 L. Additional exposure of up to hundreds of langmuirs of Cl_2 produced no further measurable increase. As shown in Fig. 3, the increase in work function with exposure to Cl closely parallels the Cl Auger signal, providing strong evidence that only a single adsorption state is present. Finally, $c(2\times2)$ features, which appeared in the LEED pattern at an intermediate coverage, reached their maximum intensity at the saturation coverage, and showed no further change with exposure.

These three observations were used to calibrate the Cl Auger signal in terms of monolayer coverage. The Auger signal is assumed proportional to the number of chlorine atoms on the surface, which should be the case for submonolayer quantities of an adsorbate occupying a single

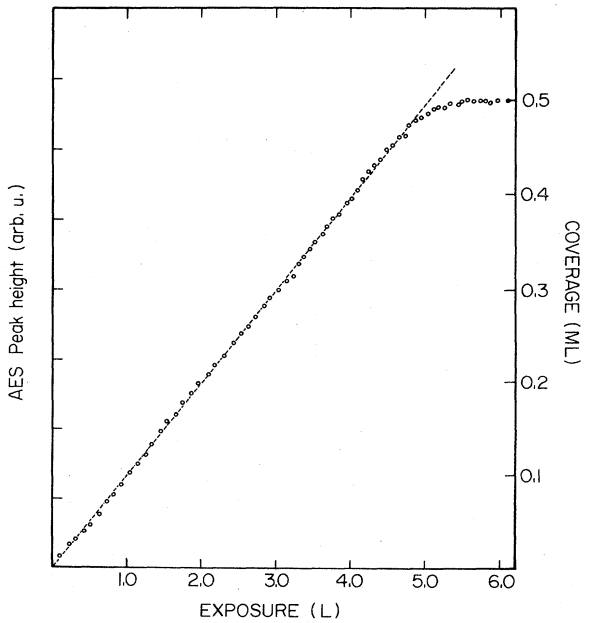

FIG. 2. The Cl Auger peak height as a function of exposure to Cl_2 at 300 K. The straight line is a least-squares fit to the data points for $\Theta < 0.4$.

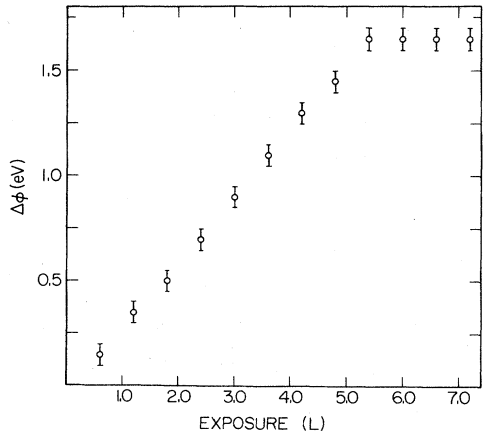

FIG. 3. The work-function change as a function of exposure to Cl_2 at 300 K.

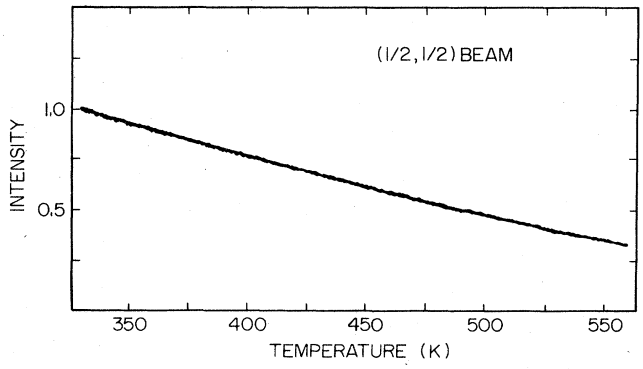

FIG. 4. The $(\frac{1}{2},\frac{1}{2})$ LEED beam height as a function of temperature at $\Theta=\frac{1}{2}$ and $E_i=66$ eV.

type of adsorption site. The optimum coverage for the $c(2\times2)$ structure is $\Theta=\frac{1}{2}$. Any additional adsorption would cause a decrease in intensity of the $c(2\times2)$ LEED beams, which was not observed even for Cl_2 pressures as high as 5×10^{-8} torr. The strength of the Cl Auger signal at saturation did not change with temperature between 300 and 600 K. Therefore we assign the low-temperature limit, $\Theta=\frac{1}{2}$, to the saturation coverage at 300 K. This results in a linear calibration of the Auger peak height to coverage as shown on the right-hand axis of Fig. 2. In addition the linear dependence of coverage on exposure can be used to determine coverages less than $\Theta\simeq0.45$. The straight line in Fig. 2 is a least-squares fit to the data with slope 0.10 ML/L.

B. Temperature dependence

To examine the temperature dependence of the $c(2\times2)$ phase boundary, we exposed the clean Ag surface at 90, 300, and 430 K to Cl_2 at 10^{-8} torr. The $c(2\times2)$ diffraction features appeared at approximately the same Cl_2 exposures (≈4 L) at all three temperatures. The quality of the Cl overlayers appeared to be temperature independent. We were able to heat a barely ordered overlayer (one with a diffuse LEED pattern) from 90 to 650 K with no perceptible change in the quality of the $c(2\times2)$ diffraction pattern. The Cl began to desorb at 650 K. The $c(2\times2)$ phase boundary thus appears to be roughly independent of temperature.

A measurement of the peak intensity of the $(\frac{1}{2},\frac{1}{2})$-order LEED beam at $\Theta=\frac{1}{2}$ versus temperature is shown in Fig. 4. There is only a gradual, smooth decrease in peak height, which is attributable to the Debye-Waller effect. We did not observe the $c(2\times2)$ overlayer to disorder upon heating until actual desorption began. Even then, the overlayer disordered only when the chlorine coverage fell below ~0.4 monolayer, i.e., below the critical coverage for ordering at any temperature. In agreement with Cardillo *et al.*[7] but in disagreement with Tu and Blakely,[3] we find no evidence for a reversible order-disorder transition above approximately 450 K.

We also find no evidence for irreversible changes in the Cl overlayer upon heating as reported by Kitson and Lambert.[14] They reported a break in the LEED I-T curve at 430 K. Our result in Fig. 4 clearly does not show such a break and also is fully reversible. Irreversible changes in the work function and the cross section for electron-stimulated desorption (ESD) following heating were also previously reported.[14] Upon heating 20 min at 500 K, we found that the work function of the Cl-saturated surface decreased by only 0.05 eV (the limit of our resolution). We tested the susceptibility of the $c(2\times2)$ chlorine overlayer (unheated) to ESD by exposing it to an electron beam of 100 μA at 1840 V for 30 min. There was a noticeable amount of ESD observed, in disagreement with Kitson and Lambert. The coverage, as measured continuously by AES, dropped steadily from $\Theta=0.5$ to $\Theta=0.37$. The coverage on other parts of the sample not touched by the electron beam was still found to be 0.5 ML after this time. We repeated this measurement under a large number of different dosing and heating procedures. The amount of ESD proved to be independent of the heating and cooling history of the sample, in complete disagreement with the previous report.[14]

C. Measurement of the phase boundary

Our detailed observations of the $c(2\times2)$ order-disorder transition consisted of measurements of the $(\frac{1}{2},\frac{1}{2})$-order LEED beam intensity profile as a function of coverage. The major problem encountered in the acquisition of these data was the accurate determination of the coverage of each profile. We used two approaches. The first was a constant-pressure technique, in which the LEED profiles were taken as a function of exposure, which was then converted to coverage. The second was a "start-stop" technique, in which a coverage was explicitly measured for each profile with AES. These two methods yielded the same results and thus served to check each other.

The constant-pressure technique took advantage of the linearity of the chlorine coverage versus exposure curve (Fig. 2). First, the photometer was focused on the position of a $(\frac{1}{2},\frac{1}{2})$-order LEED beam. One AES spectrum was then taken to determine the exact starting coverage.

(The approximate starting coverage was always about 0.30 ML.) Cl_2 at a pressure of 2×10^{-9} torr was admitted to the system, and a number of profiles were then taken evenly spaced in time. After the overlayer was ordered, the run was stopped and a second AES spectrum taken to determine the exact final coverage. Knowing the final and initial coverages, and using the demonstrated linearity of coverage versus exposure, we could then determine the coverage for each profile. The primary disadvantage of the technique was that it was difficult to regulate the chlorine gas pressure precisely.

In the start-stop technique, first a LEED profile was taken, then a coverage for the profile was measured directly with AES, and finally the sample was dosed with a very small amount of chlorine and the cycle repeated. Since we were using one set of electron optics for both LEED and AES, this technique required refocusing the electron gun and optics for each profile measured. It was thus difficult to maintain uniform experimental conditions for each profile.

Fortunately, the complementary nature of the two techniques meant that they could be used to check each other. No consistent differences could be found in the profiles generated by the two methods. We estimate the relative coverage sensitivity of both techniques to be 0.005 ML. The final data set used in our attempt to extract critical exponents consisted of 47 LEED intensity profiles spaced more-or-less evenly in coverage from 0.32 to 0.47 monolayer. All the profiles were taken at room temperature and with the same primary LEED beam energy, 66 eV. Representative profiles at coverages 0.36, 0.39, and 0.49 are shown in Fig. 5. The intensity and widths of the beam as a function of coverage are shown in Figs. 6(a) and 7. It is apparent that ordering occurs at $\Theta_c\simeq0.39$. A detailed analysis of the ordering transition is presented in Sec. IV C.

IV. ANALYSIS

A. Adsorption kinetics

The linearity of the coverage-exposure curve indicates that a simple geometrical (Langmuir) description of the sticking probability is not adequate. A coverage-invariant sticking coefficient is frequently interpreted as arising from a mobile precursor to adsorption.[15–17] The precursor is assumed to be a weakly bound molecule that can move about the surface until it either desorbs or finds an empty site for adsorption. We can fit the data of Fig. 2 well using a precursor description[15] modified to include

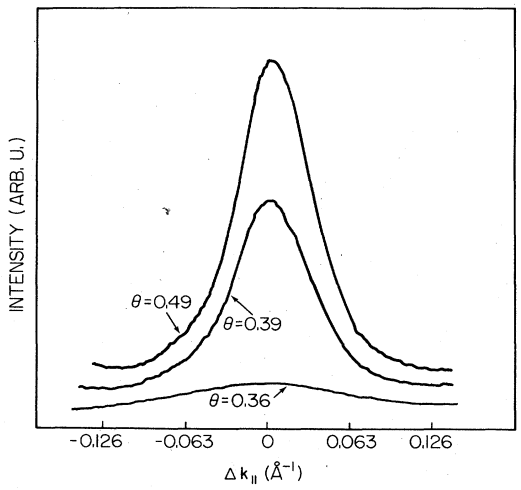

FIG. 5. Measured LEED beam profiles at $\Theta=0.36$, 0.39, and 0.49, $T=300$ K, and an incident energy of 66 eV.

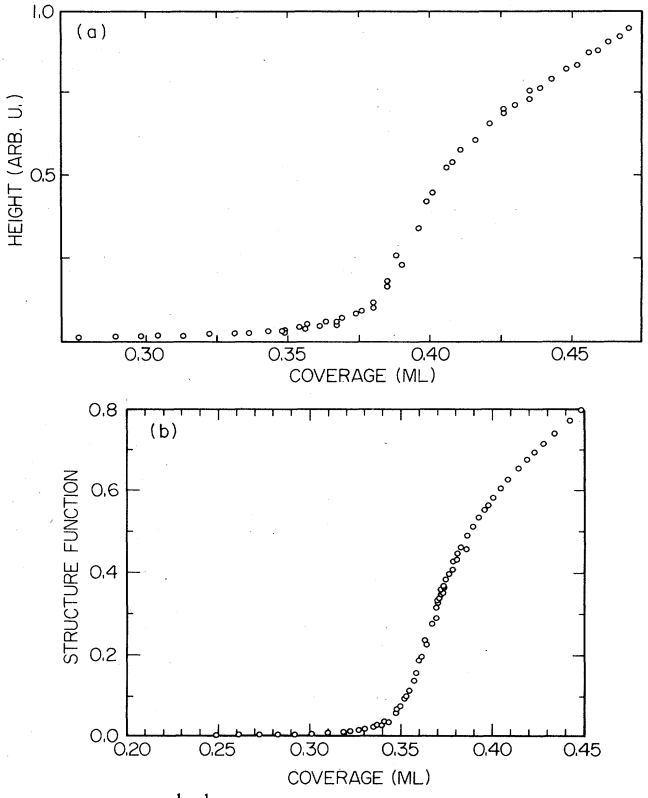

FIG. 6. The $(\frac{1}{2},\frac{1}{2})$ LEED beam height as a function of coverage. (a) Measured at 300 K, $E_i=66$ eV. (b) Calculated for the pure hard-square model using a Monte Carlo simulation on a 72×72 site lattice. Each point was obtained from runs of at least 10^5 MC steps per site.

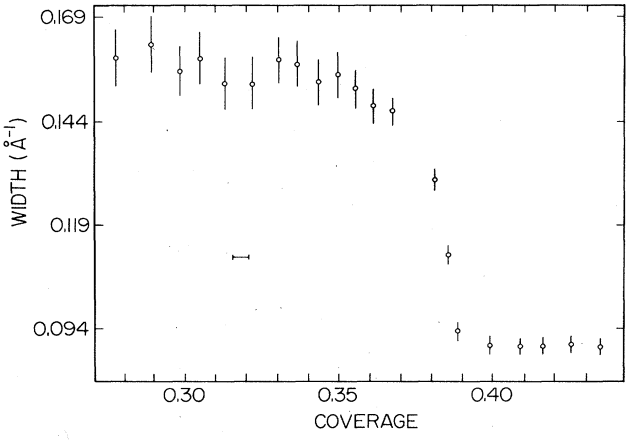

FIG. 7. The measured width of the $(\frac{1}{2},\frac{1}{2})$ LEED beam profile as a function of coverage, $T=300$ K, $E_i=66$ eV.

dissociative adsorption, if we choose the ratio of the probability of desorption from the precursor state to the probability of adsorption from the precursor state to be $\approx 2\times 10^{-3}$. The fit, however, may be fortuitous. We see little variation in the sticking coefficient with temperature, whereas a substantial variation is expected for precursor adsorption.[16,17] Other possible explanations for the coverage-independent sticking coefficient involve a cooperative motion of incoming Cl_2 molecules and adsorbed Cl atoms. The Cl_2 could be deflected toward vacant sites on the surface, or previously adsorbed Cl could move out of the path of the incoming molecule.

Previous workers have investigated the adsorption energy for Cl/Ag(100).[3] The derived isosteric heat of adsorption, q_s, is found to be roughly independent of coverage [as opposed to the strong coverage dependence of q_s measured for H/Ni(111),[18] for example]. This would occur if the Cl coverage depended only on μ/T, as in the pure hard-square model, rather than on μ and T separately. The isobars of Tu and Blakely[3] have the same form as those for the hard-square model. They are distinctly different, for example, from isobars of models where nearest-neighbor sites are significantly occupied.

B. Surface dipole

The work-function shift is linear in the coverage to saturation at $\Theta=\frac{1}{2}$ as shown in Fig. 3. From the maximum value of $\Delta\phi=1.65$ eV, the perpendicular component of the dipole moment, μ_s, can be calculated to be 0.74 D.[19] This, in turn can be used to calculate the dipole-dipole interaction energies E_{dd} at the first- and second-neighbor distances of 2.89 and 4.09 Å. The use of[20]

$$E_{dd}=2\mu_s^2/R^3 , \tag{3}$$

gives values of 28 and 10 meV for the first- and second-neighbor distances, respectively.

C. Ordering transitions and phase diagram

For the range of temperatures and pressures studied we find no evidence for the formation of nearest-neighbor pairs of Cl atoms on the surface. Adsorption stops when nearest-neighbor sites are required for an increase in coverage. There is no sign of the disordering of the saturated $c(2\times 2)$ overlayer as the temperature is increased that would occur if nearest-neighbor sites could be occupied. Furthermore, the phase boundary appears to be roughly independent of temperature. Thus the type of lattice-gas model appropriate to Cl/Ag(100) is a hard-square model, as described in the Introduction, at least for the temperatures and pressures realized in this experiment. At higher gas pressures adsorption might proceed past one-half monolayer (but perhaps at the expense of the simple two-dimensional lattice-gas picture of the surface—the strong Cl-Cl repulsions might be comparable with the Cl-Ag interactions).

A plot of the peak $c(2\times 2)$ intensity as a function of coverage is given in Fig. 6(a). For comparison Monte Carlo data for the peak intensity of the pure hard-square model on a 72×72 lattice are presented in Fig. 6(b). Recalling that the point of inflection of the curve in Fig. 6(a) represents a maximum in the specific heat,[21] we estimate the critical coverage to be 0.393 ± 0.008. The critical coverage of Cl/Ag(100) at room temperature is thus slightly greater than the critical coverage, ≈ 0.368, of the pure hard-square model.

Above the critical coverage, the scaling theory of second-order transitions predicts that the peak intensity I should be governed by the exponent β,[22]

$$I\sim(\mu-\mu_c)^{2\beta} \text{ as } \mu\rightarrow\mu_c^+ , \tag{4}$$

where μ_c is the value of the chemical potential at the critical point. This is true when the correlation length is much smaller than the size of characteristic defect-free regions on the surface and smaller than the LEED instrumental resolution. We have mimicked these two effects in our finite-size Monte Carlo simulation. The coverage is singularly related to μ:

$$(\Theta-\Theta_c)\sim(\mu-\mu_c)^{1-\alpha} . \tag{5}$$

So,

$$I\sim(\Theta-\Theta_c)^{2\beta/(1-\alpha)} . \tag{6}$$

That is, the critical exponent β has been "Fisher renormalized."[23] As the critical variation of intensity described in Eq. (6) will be superimposed on the nonsingular density variation ($I\propto\Theta^2$), we corrected our experimental intensity values [as shown in Fig. 6(a)] by a factor of Θ^2 to isolate the critical variation,

$$\frac{I}{\Theta^2}\sim(\Theta-\Theta_c)^{2\beta/(1-\alpha)} . \tag{7}$$

By plotting $\ln(I/\Theta^2)$ versus $\ln(\Theta-\Theta_c)$ and choosing Θ_c to maximize the linearity of the resulting curve, we obtain an estimate of Θ_c and $\beta/(1-\alpha)$. The best-fit log-log plot is shown in Fig. 8. We estimate that $\Theta_c=0.394\pm 0.007$ (this is the statistical uncertainty; it does not include uncertainty in the coverage calibration), and $\beta/(1-\alpha)=0.12\pm 0.03$. The value of Θ_c is consistent with the coverage at the point of inflection of Fig. 6(a). We performed the same analysis on our Monte Carlo data and

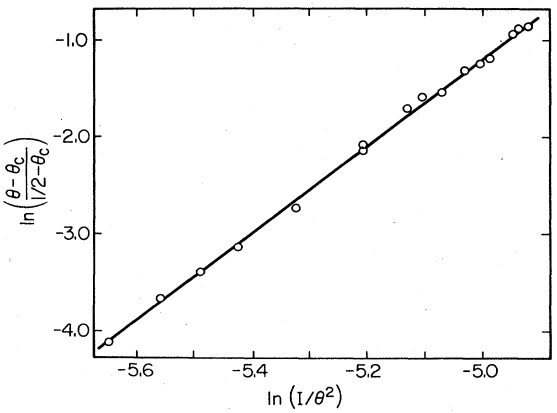

FIG. 8. Log-log plot of intensity versus the deviation from Θ_c, used for determination of $\beta/(1-\alpha)$. The solid line represents a least-squares fit to the points.

obtained the estimates $\Theta_c = 0.372 \pm 0.006$ and $\beta/(1-\alpha) \approx 0.15 \pm 0.03$. We note that most of the data used in these analyses were comparatively far from the critical point. If $T=0$ is associated with $\Theta = \frac{1}{2}$, then $(\Theta - \Theta_c)/(\frac{1}{2} - \Theta_c)$ is analogous to the reduced temperature $(T - T_c)/T_c$ of phase transitions induced by changing the temperature. The values of $(\Theta - \Theta_c)/(\frac{1}{2} - \Theta_c)$ used in the fit varied from 0.02 to 0.4 compared with the reduced temperature range of 0.02 to 0.1 used in the study of the disordering of $p(2\times2)$O/Ni(111).[24,25] The correlation length was thus small. While this justifies ignoring the effects of instrumental resolution and finite-size effects, there is no *a priori* reason to expect that the resulting effective exponents will be close to the actual exponents. That both the Monte Carlo data and experiment give exponents close to the Ising value of $\beta/(1-\alpha)$, $\frac{1}{8}$, is suggestive, however. For comparison $\beta/(1-\alpha)$ is $\frac{1}{6}$ and $\frac{1}{4}$ for the three- and four-state Potts models, respectively.[26]

The full width at half maximum of our LEED profiles is shown in Fig. 7. The critical narrowing characteristic of a divergent correlation length is evident. Because we were unable to remove the effect of the instrument on this width, it was not possible to determine the critical exponents γ and ν.

D. Implications of the lattice-gas model

To evaluate the effect of finite further-than-nearest-neighbor interactions on the hard-square phase diagram we consider second-neighbor interactions, E_2. The tricritical point, where an attractive E_2 causes a low-temperature coexistence region, is known *exactly,* as Huse[27] has observed, based on Baxter's partial solution of the generalized hard-hexagon model.[28] The tricritical temperature is $E_2/k_B \ln[(3-\sqrt{5})/4] \approx 0.60\,|E_2|/k_B$. The fact that at 90 K no coexistence region is seen thus places an approximate limit on E_2, $E_2 \gtrsim -13$ meV, independent of the coverage calibration. An exact solution of a model in statistical mechanics thus has physical implications! The phase diagram for the hard-square model with finite E_2, computed by the method described by Kinzel and Schick,[13] is shown in Fig. 9. By using this phase diagram, a transition coverage of 0.394 ± 0.007 at 300 K implies a repulsive E_2 greater than 20 meV. Kinzel and Schick show that a low-coverage 2×1 phase appears when the temperature is less than $0.30\ E_2/k_B$. That no low-coverage phase is observed at 90 K implies, *within this next-nearest-neighbor model,* that E_2 is less than 26 meV. If E_2 were 20 meV, then Θ_c would vary from 0.380 at 600 K to 0.396 at 90 K. As we have examined only the qualitative nature of the phase transition at temperatures other than 300 K we cannot rule out this type of variation in Θ_c for Cl/Ag(100).[29]

V. CONCLUSION

Chlorine adsorbed on Ag(100) forms a square-lattice gas. For the range of temperatures and pressures obtained in this experiment we found no evidence that nearest-neighboring binding sites could be simultaneously occupied; the saturation coverage appeared to be one-half monolayer and the $c(2\times2)$ Cl overlayer did not disorder when the temperature was raised to 650 K. This suggests, for the purpose of this experiment, that the Cl nearest-neighbor adatom-adatom interaction is an exclusion. The appropriate lattice-gas model is then a hard-square model. When the hard squares do not interact it is known that the $c(2\times2)$ structure continuously orders at a coverage of around 0.368 ML with Ising exponents. By making careful measurements of the $c(2\times2)$ beam LEED intensities as a function of Cl coverage (determined by Auger measurements) we determined the critical coverage of $c(2\times2)$ Cl on Ag(100) to be 0.394 ± 0.007 ML at 300 K. This difference can be explained by assuming that the hard squares, representing the Cl atoms, interact. We find that assuming a next-nearest-neighbor repulsion of 20 meV can account for all observed features of the phase diagram. The measured value of $\beta/(1-\alpha)$, 0.12 ± 0.04, is consistent with the Ising value $\frac{1}{8}$. By measuring the work-function change of the Ag surface on Cl adsorption, we conclude that the dipole-dipole contribution to the next-nearest-neighbor interaction is approximately 10 meV. So, hard-square lattice-gas models are not simply "artificial 'models' which have no counterpart in reality."[30]

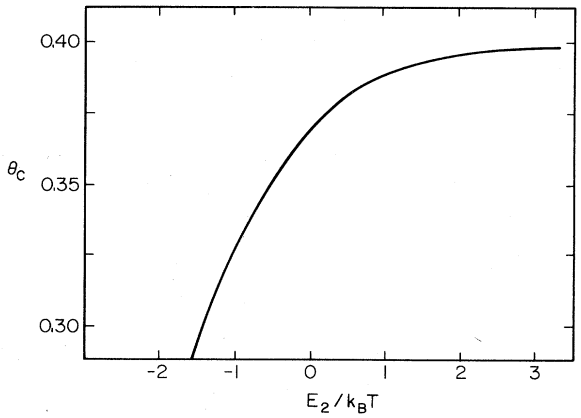

FIG. 9. Critical coverage as a function of second-neighbor interaction energy, calculated using the technique of Ref. 13.

ACKNOWLEDGMENTS

We gratefully acknowledge John F. Morar for useful discussions on instrumentation. The experimental work described here was supported by the National Science Foundation under Grant No. DMR82-04662. The theoretical work was supported by the Department of Energy under Grant No. DE-FG05-84ER45071. Computer facilities were supplied by the University of Maryland Computer Science Center.

*Present address: Physical Review, 1 Research Road, Box 1000, Ridge, NY 11961.
†Author to whom correspondence should be addressed.

[1]C. Davisson and L. H. Germer, Phys. Rev. **30**, 705 (1927).
[2]G. A. Somorjai and M. A. Van Hove, *Adsorbed Monolayers on Solid Surfaces* (Springer, Berlin, 1979).
[3]Y. Tu and J. M. Blakely, Surf. Sci. **85**, 276 (1979).
[4]G. Rovida and F. Pratesi, Surf. Sci. **51**, 270 (1975).
[5]S. P. Weeks and J. E. Rowe, J. Vac. Sci. Technol. **16**, 470 (1979).
[6]E. Zanazzi, F. Jona, D. W. Jepson, and P. M. Marcus, Phys. Rev. B **14**, 432 (1976).
[7]M. J. Cardillo, G. E. Becker, D. R. Hamann, J. A. Serri, L. Whitman, and L. F. Mattheiss, Phys. Rev. B **28**, 494 (1983).
[8]D. J. Gaunt and M. E. Fisher, J. Chem. Phys. **43**, 2840 (1965).
[9]R. J. Baxter, I. G. Enting, and S. K. Tsong, J. Stat. Phys. **22**, 465 (1980).
[10]D. W. Wood and M. Goldfinch, J. Phys. A **13**, 2781 (1980).
[11]Z. Racz, Phys. Rev. B **21**, 4012 (1980).
[12]F. H. Ree and D. A. Chesnut, J. Chem. Phys. **45**, 3983 (1966).
[13]W. Kinzel and M. Schick, Phys. Rev. B **24**, 324 (1981).
[14]M. Kitson and R. M. Lambert, Surf. Sci. **100**, 368 (1980).
[15]P. Kisliuk, J. Phys. Chem. Solids **3**, 95 (1957).
[16]D. A. King and M. G. Wells, Proc. R. Soc. London, Ser. A **339**, 245 (1974).
[17]M. Shayegan, J. M. Cavallo, R. E. Glover III, and R. L. Park, Phys. Rev. Lett. **53**, 1578 (1984).
[18]K. Christmann, O. Schober, G. Ertl, and M. Neumann, J. Chem. Phys. **60**, 4528 (1979).
[19]G. Ertl and J. Küppers, *Low Energy Electrons and Surface Chemistry* (Verlag Chemie, Weinheim, 1974).
[20]W. Kohn and K. H. Lau, Solid State Commun. **18**, 553 (1976).
[21]N. C. Bartelt, T. L. Einstein, and L. D. Roelofs, Surf. Sci. **149**, L47 (1985), and Phys. Rev. B **32**, 2993 (1985).
[22]For example, H. E. Stanley, *Introduction to Phase Transitions and Critical Phenomena* (Oxford University Press, New York, 1971).
[23]M. E. Fisher, Phys. Rev. **176**, 257 (1968).
[24]L. D. Roelofs, A. R. Kortan, T. L. Einstein, and R. L. Park, Phys. Rev. Lett. **46**, 1465 (1981).
[25]A. R. Kortan and R. L. Park, Phys. Rev. B **23**, 6340 (1981).
[26]F. Y. Wu, Rev. Mod. Phys. **54**, 235 (1982).
[27]D. A. Huse, Phys. Rev. Lett. **49**, 1121 (1982).
[28]R. J. Baxter, J. Phys. A **13**, L61 (1980).
[29]R. Q. Hwang, E. D. Williams, and R. L. Park, Bull. Am. Phys. Soc. **30**, 335 (1985).
[30]J. M. Ziman, *Models of Disorder* (Cambridge University Press, Cambridge, 1979).